

# A Validated Cohesive Finite Element Analysis of Needle Insertion into Human Skin

H. Mohammadi<sup>1</sup> and N. Maftoon<sup>1</sup>

<sup>1</sup> Department of Systems Design Engineering, University of Waterloo, Waterloo, Canada

**Abstract**— Medical needles play important roles in many diagnostic and therapeutic applications and the development of novel surgical technologies depends on obtaining a better quantitative description of needle-tissue interactions. To develop such technologies involving needles, the investigation of the needle insertion process and the related parameters are key. This paper provides a two-dimensional finite element model of needle insertion into the human skin, validated against available experimental results in the literature. The crack propagation in the tissue was modelled via the cohesive zone method. To this end, a curve-fitting approach based on the reaction force applied to the needle during the insertion was exploited to optimize cohesive parameters. The simulations showed that failure traction of 2 MPa, initial stiffness of 4000 MPa/mm, and separation length of 1.6 mm can lead to a reliable model that can reproduce the experimental results. Also, the effect of needle diameter on the insertion force was investigated.

**Keywords**— Needle Insertion, Finite Element, Cohesive Zone

## I. INTRODUCTION

Developing new surgical technologies and improving the design of the medical equipment can lead to safer and more convenient medical procedures and can even enable expansion of medical services to regions with limited access. Needles are among the most applicable clinical devices that are frequently used for vaccination, drug delivery, brachytherapy, biopsy, and different types of surgeries [1], [2]. Therefore, the investigation of needle-tissue interactions can inform the development of more efficient and controlled apparatus for medical procedures.

The pain level that each patient tolerates can be moderated by improvements in the needle design in terms of its diameter and tip angle to reduce the insertion force of the needle [3], [4]. Additionally, the insertion force varies by the mechanical properties of the human skin, which depends on different parameters such as gender, age, anatomical location, and ethnicity [5].

The mechanical properties that take part in the needle-skin interactions are categorized into three classes of parameters to develop a complete model: (1) deformation-related parameters, (2) fracture-related parameters, and (3) needle-skin interaction parameters. The first class depends on the stress-strain characteristics of the skin, which is governed by the

constitutive laws. Although elastic models have been frequently used in the determination of stress-strain relationships in several studies, more complicated models like viscoelastic and hyperelastic models have shown more reliable results [6]. The second class includes parameters like fracture toughness, critical strain energy release rate, and crack tip opening displacement that can be used to describe the fracture in the skin. Nevertheless, approaches like the Cohesive Zone (CZ) method may use some other equivalent parameters to describe crack propagation. Finally, the third class contains the frictional characteristics of the skin along with its contact pressure-overclosure definition.

Finite Element (FE) method has been frequently used for the simulation of needle insertion into biological tissues. However, only very few studies could provide experimentally validated FE models of needle insertion into the human skin. Kong et al. [2] simulated microneedle insertion into a multilayer human skin until the earliest stages of skin penetration and verified their results with the experimental results reported in [7]. Chen et al. [8] developed a FE model of the insertion of microneedles into the mouse skin using an element deletion strategy based on the ultimate strength of the skin. Also, Halabian et al. [1] simulated the needle-skin interaction to study the stress fields and the skin deformation before the deep penetration of the needle.

In this study, a two-dimensional FE model was developed using the CZ method to simulate deep needle insertion into the human skin. This model was validated using the needle reaction force data obtained experimentally by Shergold and Fleck [9]. Also, the effects of cohesive parameters and needle diameter on the reaction force were studied. This study provides a better understanding of the mechanics of needle insertion into the human skin, which can culminate in the design of more advanced medical devices or the improvement of needle insertion control in robot-assisted surgery and virtual-reality based medical training systems.

## II. METHODOLOGY

### A. Mechanics of Needle insertion

Any cutting process is associated with a certain level of energy consumption. Needle insertion into the skin is a cutting process in which energy consumption is composed of

three different mechanical phenomena: skin deformation, crack propagation, and needle-skin friction. Consequently, the external work during the insertion is equivalent to the combination of three components:

$$W_{\text{ext}} = U_s + U_{G_c} + U_f \quad (1)$$

where  $W_{\text{ext}}$  is the total external work done by the needle,  $U_s$  is strain energy in the skin and subcutaneous tissue due to deformation,  $U_{G_c}$  is the fracture energy owing to crack propagation, and  $U_f$  is the frictional energy because of the interaction of the needle with the skin.

The CZ method was implemented in the current study to model the damage in the human skin and simulate crack propagation during the needle insertion. A very thin ( $10 \mu\text{m}$ ) cohesive layer in the skin, parallel to the direction of needle insertion was assumed. During the insertion, the cohesive layer opens, and its surfaces take apart.

The mechanical properties of the cohesive elements are described by a traction-separation law (TSL), which defines the traction ( $t$ ) between cohesive surfaces versus the separation distance ( $\delta$ ). In the current study, a bilinear TSL as shown in Figure 1 was used to define cohesive interactions. The traction of the cohesive surfaces increases linearly up to a maximum traction known as the failure traction ( $t_c$ ) and then gradually degrades to zero at which the total surface energy (the area under curve) accumulates to the fracture toughness in terms of strain energy density,  $G_c$ . It is also noticeable that the initial stiffness ( $K$ ) is usually large enough to allow the continuity of the skin structure.

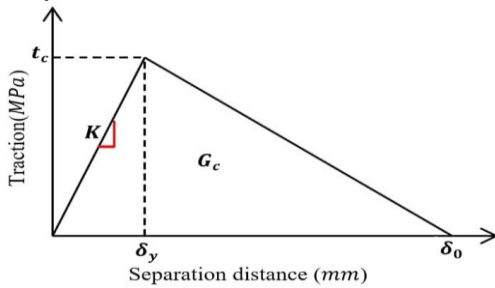


Fig. 1. CZ method; a) needle insertion into the cohesive elements, b) traction-separation law (TSL)

### B. Two-dimensional FE model

The proposed model aimed to observe the skin cutting along the needle insertion trajectory. Therefore, a limited part of the skin and subcutaneous tissue around the penetration path was modelled. Thus, the model consisted of the skin layer, subcutaneous layer, and the needle as illustrated in Figure 2. The geometrical parameters of the model, which correspond with the experimental measurements performed by Shergold and Fleck [9], are presented in Table 1.

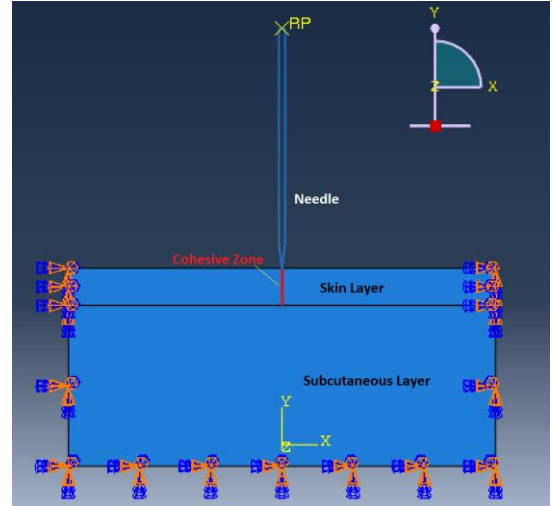


Fig. 2. FE model consisting of needle, skin layer, and subcutaneous layer

Table 1. Geometrical parameters used in the FE model

Geometrical parameter	Symbol	Size
Needle diameter	$d$	0.6 mm
Needle tip angle	$\theta$	14 degrees
Skin thickness	$t_{\text{skin}}$	3.5 mm
Subcutaneous layer depth	$t_{\text{sub}}$	15 mm
Boundary condition lateral distance	$L$	20 mm

The needle was considered to be rigid because it was made of stainless steel and it was much stiffer than skin. An incompressible, isotropic, and 1<sup>st</sup> order Ogden hyperelastic model with the following strain energy density function was chosen for the skin layer:

$$\varphi(\lambda_1, \lambda_2, \lambda_3) = \frac{2\mu}{\alpha^2} (\lambda_1^\alpha + \lambda_2^\alpha + \lambda_3^\alpha - 3) \quad (2)$$

where  $\lambda_i$  ( $i = 1, 2, 3$ ) are the principle stretches and  $\mu$  and  $\alpha$  are the Ogden constants, which were considered 0.11 MPa and 9, respectively, as reported in [9]. Furthermore, a simple linear elastic model, with the Young's modulus of 0.5 MPa, which is in the range of reported values in [10], was considered for the subcutaneous tissue. Also, since the subcutaneous tissue is almost incompressible, a Poisson's ratio of 0.49 was implemented in the proposed model [11]. The damage mechanism in the skin layer was established based on the CZ model presented in Section II-A and a hard contact between the needle and skin with a penalty friction formulation was defined. Because previous investigations pointed out that the required force for penetration in the subcutaneous layer is negligible [9], this model did not include any interaction be-

tween the needle and subcutaneous tissue to reduce the computational expense. All external boundaries in either the skin or subcutaneous layers were fixed, except the top surface of the skin which was free. The boundary conditions were defined far enough away from the insertion point that eliminated the effect of boundary conditions on the reaction force and stress fields around the crack tip.

Simulations were performed in Abaqus V2020 (Dassault Systèmes, MA, United States). The skin and subcutaneous layers were meshed with 3-node linear plane strain triangle elements (CPE3), and 4-node bilinear plane strain quadrilateral elements with reduced integration (CPE4R), respectively. Moreover, the elements of CZ along the trajectory of needle insertion were 4-node two-dimensional cohesive elements (COH2D4). A mesh convergence study was performed to ensure the accuracy of the numerical simulations.

### III. RESULTS AND DISCUSSIONS

#### A. Cohesive Parameters

The fracture mechanics of the skin has not been investigated profoundly in the literature. Consequently, there are lots of ambiguities in fracture-related parameters of the skin. Previous studies have shown that the fracture toughness of skin in needle-insertion experiments depends on the insertion velocity and more importantly the needle diameter [12]. The cohesive parameters of the proposed model were optimized to replicate experimental insertion measurement data performed with a needle of 0.6 mm diameter and insertion rate of 1 mm/s [9]. Also, the friction coefficient during the needle insertion into the skin was considered in the optimization procedure.

Figure 3 shows the effect of cohesive parameters of the FE model on the insertion force of a needle with a diameter of 0.6 mm and insertion velocity of 1 mm/s. The CZ model with the failure traction ( $t_c$ ) of 2 MPa, initial stiffness ( $K$ ) of 4000 MPa/mm, and separation length ( $\delta_0$ ) of 1.6 mm using a friction coefficient of 0.05 (red) could replicate the experimental data (blue) most closely (RMSE = 0.12 N). The parameters  $t_c$  and  $\delta_0$  indicate a fracture toughness of 1.6 MPa.mm, which is very similar to the fracture toughness of the human hand skin (1.7 MPa.mm) reported in [13] and corresponds with the fracture toughness of the porcine skin (1.6 MPa.mm) interpolated for the insertion rate of 1 mm/s and needle diameter of 0.6 mm [12].

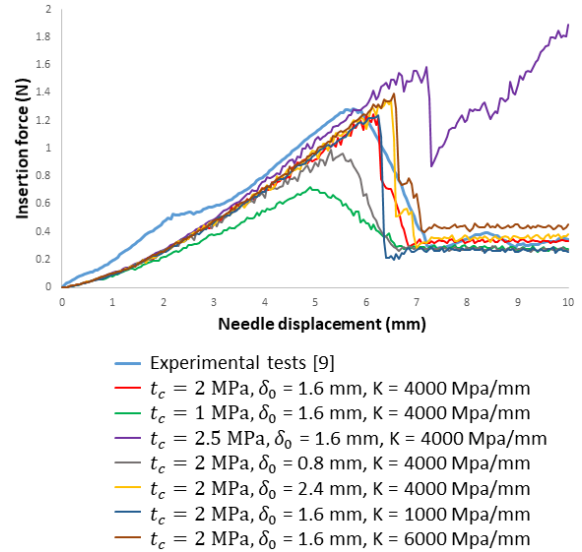


Fig. 3. The effect of failure traction ( $t_c$ ), separation length ( $\delta_0$ ), and initial stiffness ( $K$ ) on the insertion force

The investigation of cohesive parameters in Figure 3 shows that  $t_c$  was the most influential parameter while  $K$  had the least effect on the reaction force of the needle. Because increasing  $t_c$  and  $\delta_0$  increased the fracture toughness, the energy required for creating new crack surfaces escalated. On the other hand, changing  $K$  just altered the initial stiffness of CZ and did not have any significant impact on the required energy. This energy description explains why  $t_c$  and  $\delta_0$  have more significant effects on the insertion force.

#### B. Geometrical Parameters

It has been shown that the stress concentration in a segment of tissue is an acceptable interpretation of patients' pain [1]. The results of the current study showed that the stress value at the insertion point increases with the needle insertion force, which is highly affected by the needle geometry. A parameter study on the effect of needle diameter on the insertion force was performed. Figure 4 displays the alteration of the insertion force for different diameters. Increasing the needle diameter led to larger insertion forces in deeper penetration values. In particular, increasing the needle diameter from 0.19 mm to 0.99 mm escalated the insertion force from 0.22 N to 2.17 N. Moreover, for thicker needles, the thorough penetration of the needle into the skin layer occurred later in larger displacement values. The proposed model can also be optimized based on the patients' skin thickness and mechanical properties to find the insertion force and displacement at the puncture point for each specific case.

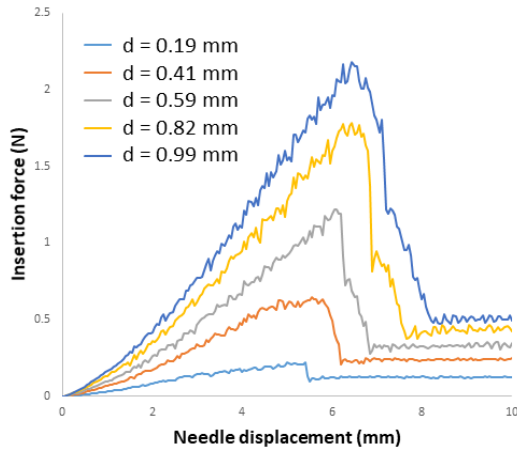


Fig. 4. The effect of needle diameter ( $d$ ) on the insertion force

#### IV. CONCLUSIONS

This study proposed a two-dimensional FE model using cohesive elements to simulate the deep penetration of a needle into the skin. The parameters of the traction-separation law that are used in the definition of CZ are optimized based on the experimental measurement data of needle insertion into the human skin. The FE model fitted suitably with the experimental results (RMSE = 0.12 N) using a failure traction ( $t_c$ ) of 2 MPa, initial stiffness ( $K$ ) of 4000 MPa/mm, and separation length ( $\delta_0$ ) of 1.6 mm.

The effect of needle diameter on the insertion force was investigated. The results showed that thinner needles require less pushing force for thorough penetration. The model developed in this research can be used for optimizing the procedures that involve medical needles, developing new therapeutic solutions, and improving the precision of medical robotic systems.

#### ACKNOWLEDGMENT

This work was supported by the Natural Sciences and Engineering Research Council of Canada (NSERC).

#### CONFLICT OF INTEREST

The authors declare that they have no conflict of interest.

#### REFERENCES

- [1] M. Halabian, B. Beigzadeh, A. Karimi, H. A. Shirazi, and M. H. Shaali, 'A combination of experimental and finite element analyses of needle-tissue interaction to compute the stresses and deformations during injection at different angles', *J. Clin. Monit. Comput.*, vol. 30, no. 6, pp. 965–975, Dec. 2016, doi: 10.1007/s10877-015-9801-9.
- [2] X. Q. Kong, P. Zhou, and C. W. Wu, 'Numerical simulation of microneedles' insertion into skin', *Comput. Methods Biomech. Biomed. Engin.*, vol. 14, no. 9, pp. 827–835, Sep. 2011, doi: 10.1080/10255842.2010.497144.
- [3] D. J. van Gerwen, J. Dankelman, and J. J. van den Dobbelsteen, 'Needle-tissue interaction forces – A survey of experimental data', *Med. Eng. Phys.*, vol. 34, no. 6, pp. 665–680, Jul. 2012, doi: 10.1016/j.medengphy.2012.04.007.
- [4] A. M. Okamura, C. Simone, and M. D. O'Leary, 'Force Modeling for Needle Insertion Into Soft Tissue', *IEEE Trans. Biomed. Eng.*, vol. 51, no. 10, pp. 1707–1716, Oct. 2004, doi: 10.1109/TBME.2004.831542.
- [5] S. Luebberding, N. Krueger, and M. Kerscher, 'Mechanical properties of human skin *in vivo* : a comparative evaluation in 300 men and women', *Skin Res. Technol.*, vol. 20, no. 2, pp. 127–135, May 2014, doi: 10.1111/srt.12094.
- [6] H. Joodaki and M. B. Panzer, 'Skin mechanical properties and modeling: A review', *Proc. Inst. Mech. Eng. [H]*, vol. 232, no. 4, pp. 323–343, Apr. 2018, doi: 10.1177/0954411918759801.
- [7] S. P. Davis, B. J. Landis, Z. H. Adams, M. G. Allen, and M. R. Prausnitz, 'Insertion of microneedles into skin: measurement and prediction of insertion force and needle fracture force', *J. Biomech.*, vol. 37, no. 8, pp. 1155–1163, Aug. 2004, doi: 10.1016/j.jbiomech.2003.12.010.
- [8] J. Chen, N. Li, and S. Chen, 'Finite element analysis of microneedle insertion into skin', *Micro Nano Lett.*, vol. 7, no. 12, pp. 1206–1209, Dec. 2012, doi: 10.1049/mnl.2012.0585.
- [9] O. A. Shergold and N. A. Fleck, 'Experimental Investigation Into the Deep Penetration of Soft Solids by Sharp and Blunt Punches, With Application to the Piercing of Skin', *J. Biomech. Eng.*, vol. 127, no. 5, p. 838, 2005, doi: 10.1115/1.1992528.
- [10] K. Comley and N. A. Fleck, 'A micromechanical model for the Young's modulus of adipose tissue', *Int. J. Solids Struct.*, vol. 47, no. 21, pp. 2982–2990, Oct. 2010, doi: 10.1016/j.ijsolstr.2010.07.001.
- [11] H. Ou, P. Zhan, L. Kang, J. Su, X. Hu, and S. Johnson, 'Region-specific constitutive modeling of the plantar soft tissue', *Biomech. Model. Mechanobiol.*, vol. 17, no. 5, pp. 1373–1388, Oct. 2018, doi: 10.1007/s10237-018-1032-9.
- [12] A. C. Barnett, Y.-S. Lee, and J. Z. Moore, 'Needle geometry effect on vibration tissue cutting', *Proc. Inst. Mech. Eng. Part B J. Eng. Manuf.*, vol. 232, no. 5, pp. 827–837, Apr. 2018, doi: 10.1177/0954405416654188.
- [13] B. P. Pereira, P. W. Lucas, and T. Swee-Hin, 'Ranking the fracture toughness of thin mammalian soft tissues using the scissors cutting test', *J. Biomech.*, vol. 30, no. 1, pp. 91–94, Jan. 1997, doi: 10.1016/S0021-9290(96)00101-7.

#### Corresponding author:

Author: Nima Maftoon  
 Institute: University of Waterloo  
 Street: 200 University Avenue  
 City: Waterloo  
 Country: Canada  
 Email: nmaftoon@uwaterloo.ca